PERGAMON

Journal of Structural Geology 23 (2001) 1415–1428

JOURNAL OF STRUCTURAL GEOLOGY

www.elsevier.com/locate/jstrugeo

Development of symmetrical and asymmetrical fabrics in sheet-like igneous bodies: the role of magma flow and wall-rock displacements in theoretical and natural cases

L.C. Correa-Gomes[a,b,*], C.R. Souza Filho[a], C.J.F.N. Martins[c], E.P. Oliveira[a]

[a]*Instituto de Geociências, University of Campinas, P.O. Box 6152, 13083-970, Campinas, SP, Brazil*
[b]*Centro Federal de Educação Tecnológica da Bahia /Universidade Católica do Salvador, Salvador, BA, Brazil*
[c]*Instituto de Geociências, Universidade Federal da Bahia, Brazil*

Abstract

Two orientations of fabrics are recognised in vertical dykes: a symmetric orientation associated with magma injected into non-deforming wall-rocks and an asymmetric orientation usually associated with external non-coaxial shearing, or magma injected into an active fault. The notion of two fabric arrangements stems from two planes of symmetry, the dyke symmetry plane (DSP) and the fabric symmetry plane (FSP). This paper uses conceptual models to simulate all possible orientations of magma flow indicators that might be produced within a vertical dyke emplaced under coeval internal and external stresses. The effect of magmatic buoyancy-related stresses are portrayed in terms of magma flow velocities (MFV) and the external non-coaxial tectonic-related stresses in terms of wall displacement velocities divided by two (WMV/2). The tectonic setting is that of a sinistral transcurrent fault.

Using these assumptions, five cases are proposed: MFV $\gg$ WDV/2, MFV $>$ WDV/2, MFV $=$ WDV/2, MFV $<$ WDV/2 and MFV $\ll$ WDV/2. Each of theses cases shows distinct obliquities between the DSP and FSP (to the extent that the latter can be depicted) and distinct angular relations between strikes of dyke walls and fabric ellipsoids. The model was tested on Neoproterozoic alkaline dykes hosted within the Itabuna–Itaju do Colonia Shear Zone (Brazil). Comparisons of what our model predicted with what we observed in the field showed a striking equivalence. © 2001 Published by Elsevier Science Ltd.

1. Introduction

The kinematics of formation of rock structures—that is, the displacements that have occurred in producing them—are expressed by the geometries, distributions and preferred orientations of crystals and clasts, here referred to as fabrics and subfabrics (Fernandez and Laporte, 1991). Fabrics may also contribute to the understanding of forces that were active along with other geologic processes (i.e. paleostresses). The arrangements of fabrics that provide information on the sense of shear (i.e. kinematic indicators) and the shapes of strain (e_1, e_2 and e_3 axes) and fabric (Λ_1, Λ_2 and Λ_3 axes) ellipsoids within rocks that were submitted to deviatoric stresses (e.g. shear zones) is fairly well understood. The subject has received considerable attention in the last three decades (Fig. 1a; Ghosh and Ramberg, 1976; Ramsay, 1980; Simpson and Schmid, 1983; Passchier and Simpson, 1986; Hanmer and Passchier, 1991; Hippert, 1993; Passchier, 1994, among others).

In igneous rocks, magmatic fabrics are reported as the preferred dimensional orientations (PDO), shape preferred orientations (SPO) and lattice preferred orientations (LPO) of particles (Blumenfeld and Bouchez, 1988; Benn and Allard, 1989; Fernandez and Laporte, 1991; Ildefonse et al., 1992). Finite arrangements and shapes of magmatic fabrics are controlled mainly by: (i) the viscosity contrast between markers and matrix, (ii) the aspect ratios of the markers (or crystals), (iii) their initial distribution/concentration, and (iv) the deformation history (or magma flow) (Gay, 1968; Fernandez and Laporte 1991; Ildefonse et al., 1992). In low symmetry fabrics (e.g. monoclinic patterns) obliquities between C–S, S–S' foliations and different mineral subfabrics (e.g. feldspars and micas) and tiling of megacrysts were used to provide a criterion for determination of the magmatic shear sense (Blumenfeld and Bouchez, 1988; Benn and Allard, 1989; Fernandez and Laporte, 1991).

In sheet-like igneous bodies (e.g. dykes) the study of the

* Corresponding author. Present address: Rua Emidio Santos s/n, Barbalho, 40300-010 Salvador, BA, Brazil. Tel.: +55-19-37884576, fax: +55-19-32891097.

E-mail addresses: gomes@ige.unicamp.br (L.C. Correa-Gomes), beto@ige.unicamp.br (C.R. Souza Filho).

0191-8141/01/$ - see front matter © 2001 Published by Elsevier Science Ltd.
PII: S0191-8141(01)00007-4

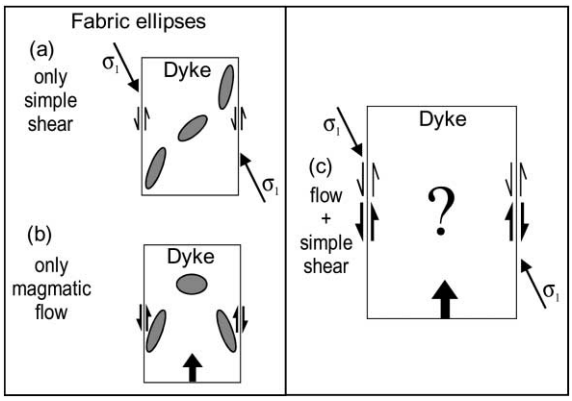

Fig. 1. Known geometry and distribution of fabric ellipses (Λ_1–Λ_3; Fernandez and Laporte, 1991) for two model end-members: (a) strain due to external shear stress (simple shear) only, or magma injected into an active fault; (b) strain due to magmatic flow (assuming Newtonian magma–linear-viscous flow) only, or magma injected into non-deforming wallrocks (Johnson and Pollard, 1973a,b; Blanchard et al., 1979; Blumenfeld and Bouchez, 1988). The results of combining both types of stress field (c) are poorly constrained.

kinematics involved in fluid-state flow of magma is relatively more restricted (Fig. 1b; Blanchard et al., 1979; Shelley, 1985; Baer and Reches, 1987; Smith, 1987; Doblas et al., 1988; Knight and Walker, 1988; Rickwood, 1990; Philpotts and Asher, 1994; Baer, 1995). The structures most likely to be useable for determination of magma flow directions vary with the magma composition. For many cases, macroscopic features like scour marks and tiling of phenocrysts and xenoliths as well as anisotropy of magnetic susceptibility (AMS) ellipsoids are the most useful criteria (Smith, 1987; Knight and Walker, 1988; Rickwood, 1990; Philpotts and Asher, 1994; Baer, 1995). The arrangement of such magmatic flow indicators is usually studied, taking into account only the stress field directly related to magma driving pressure (Fig. 1b; Blanchard et al., 1979; Shelley, 1985; Rickwood, 1990; Baer 1995), that is defined as the magma buoyancy pressure (P_m) minus the minimum compressive host-rock stress (σ_3) (Pollard, 1987; Hoek 1995). Non-coaxial shear is generally considered to be the dominant kinematic flow type in shallow intrusive rocks and magma transport (Shelley, 1985; Blumenfeld and Bouchez, 1988), though two-stage non-coaxial and coaxial shear models have also been envisaged (Smith et al., 1994). A key point of interest and debate is the extent to which fabrics within a dyke are developed only due to this magma buoyancy-related stress. The literature is relatively scanty on papers that attempt to tackle the mechanics of dyke emplacement in active, non-coaxial shear zones. Such complex scenarios involve emplacement under both external and internal stress fields (Fig. 1c).

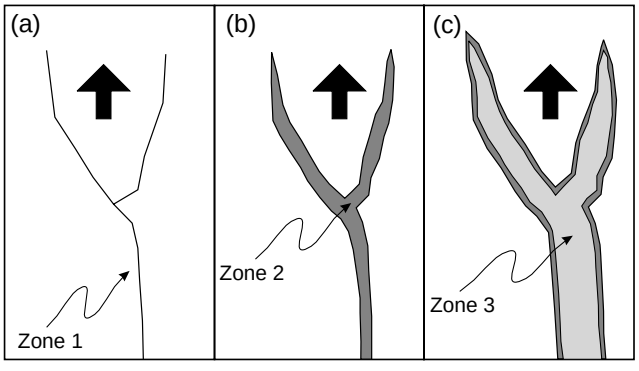

Fig. 2. The three main stages of dyke emplacement. (a) Evolution of a leading fracture system (zone 1); (b) propagation of dyke-tip magma (zone 2); (c) main magma flow (zone 3) (modified from Baer (1995)). Arrows represent fracture-conduit propagation and magmatic flow direction.

Here we attempt to use conceptual models to simulate all possible orientation of magma flow fabrics that might be produced within a vertical dyke emplaced under coeval internal (lateral magmatic flow) and external non-coaxial (tectonic, sinistral transcurrent) stresses, testing predictions derived from the models against field observations.

2. Conceptual model

2.1. Initial constraints

The emplacement of dykes involves mainly three interrelated stages (Baer, 1995): (i) propagation of a leading fracture system ahead of the dyke-tip, (ii) propagation of dyke-tip fluids, and (iii) magma flow within the dyke.

These stages and intrinsic processes yield the final configuration of a dyke (Fig. 2), which can be envisaged as three main zones: (i) an exterior shell that controls and outlines the dyke's overall geometry (zone 1), (ii) an intermediate shell that comprises the initial stages of magma intrusion, generally associated with development of chilled margins (zone 2), and (iii) a core zone comprising the main magma flow (zone 3).

Many magma flow fabrics are concentrated within zone 3 of sheet-like igneous bodies (Rickwood, 1990; Baer, 1995). There, in our conception, fabrics may be governed essentially by two types of stress field: (i) an internal stress field that is a function exclusively of the magma buoyancy pressure and, (ii) an external stress field related to local shear (tectonic) stress and host rock failure strength (Fig. 1).

Magma-related velocity profiles develop as a function of modelled magma rheological behaviours. These can be mainly: (i) Newtonian (linear viscous); (ii) pseudo-plastic, or (iii) Bingham (visco-plastic) (Shaw, 1969; Johnson and Pollard, 1973a,b; Blanchard et al., 1979) (Fig. 3). During magma flow, velocity gradient differences induce non-coaxial shear parallel to the flow plane in an opposite sense in each side of the dyke. The shear intensity decreases progressively from the margins towards the dyke center. On the dyke center, a minimum shear strain zone, where magma reaches its highest velocity, is formed (Blanchard et al.,

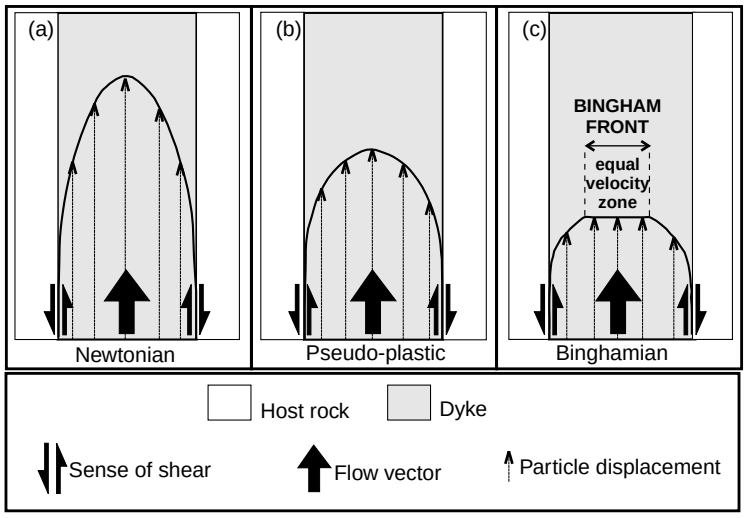

Fig. 3. Model velocity profiles for three typical magma behaviors: (a) Newtonian or linearly viscous; (b) pseudo-plastic; (c) Bingham or visco-plastic (Shaw 1969; Johnson and Pollard 1973a,b; Blanchard et al., 1979). The shape differences in each of the profiles correspond to variations in the magma internal cohesion.

1979; Merle, 1998). Therefore, velocity gradient differences draw the geometry of the velocity profiles. Variations among such profiles are controlled, for example, by changes in the volumetric proportion of particle/liquid/volatile within the magma flow (Shaw et al., 1968) and strain rates (Vigneresse et al., 1996). Shape contrasts among these profiles indicate an increase in magma internal cohesion from the Newtonian to the Bingham behavior (Johnson and Pollard, 1973a,b), which is accompanied by an increase in particle transport, blocking effects, polymerization and mechanical interactions between particles in the same direction (Shaw et al., 1968; Elston and Smith, 1970; Blanchard et al., 1979), with markers rapidly losing their ciclicity (Arbaret et al., 1996).

Fabrics, or the bulk of preferred orientations of kinematic markers (Fernandez and Laporte, 1991), are represented by the fabric ellipsoid, which is composed of three average orientation principal axes, mutually orthogonals: the maximum axis (Λ_1), the secondary axis (Λ_2) and the minimum axis (Λ_3) (Fernandez and Laporte, 1991). The axes of ellipsoidal strained phenocrysts, clasts and xenoliths can, therefore, be estimated in relation to the kinematics of magmatic flow. Due to lateral magmatic shearing, particles are rotated and tend to align parallel to the flow direction and close to dyke walls, forming angles of 10–30° with the flow plane (Blanchard et al., 1979, Blumenfeld and Bouchez, 1988; Benn and Allard 1989). In dykes, this arrangement is symmetric wall-to-wall and usually the acute angles point towards the opposite direction to the magma source (Blanchard et al., 1979; Rickwood, 1990; Baer, 1995). A remarkable exception to this, however, is when deformation is intense enough to rotate foliations past the flow plane, inducing a wrong sense of shear to be determined (Blumenfeld and Bouchez, 1988; Benn and Allard, 1989; Fernandez and Laporte, 1991).

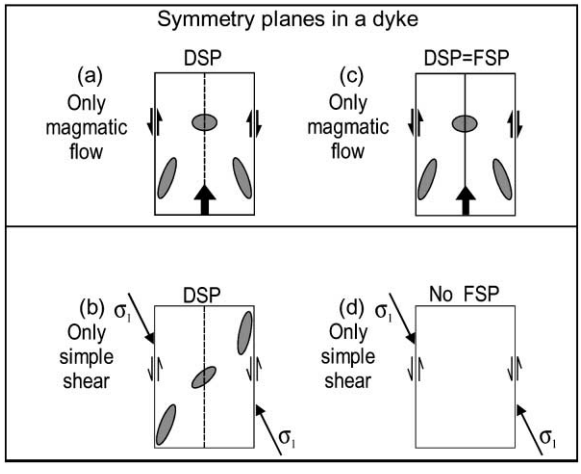

Fig. 4. Planes of symmetry in dykes for geometric and kinematic analysis. DSP = dyke symmetry plane (DSP) (i.e. the plane that divides the dyke longitudinally in two equal parts). FSP = fabric symmetry plane (i.e. the bisector of fabric mean orientations near the two dike walls).

Considering a hypothetical vertical dyke and the presence of magma flow indicators within zone 3 (Fig. 2c), it is important to conceive two planes of symmetry for geometric and kinematic analysis. One plane 'splits' the dyke longitudinally into two equal parts, i.e. the dyke symmetry plane (DSP) (Fig. 4a and b). The other reference plane is the bisector of fabric mean orientations near the two dyke walls (a plane that bisects internal fabrics in two equal fabric (Λ_1–Λ_2) clusters), i.e. the fabric symmetry plane (FSP) (Fig. 4c and d).

Bearing in mind these planes of symmetry, magma flow fabrics within the dyke zone 3 may show two possible arrangements in relation to the DSP: symmetrical and asymmetrical. Symmetrical fabrics in relation to the DSP may be produced from the shearing induced by the magmatic flow

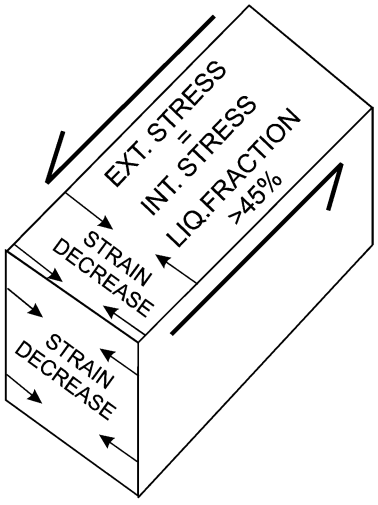

Fig. 5. Simplifying assumptions implied in the model: (i) the liquid fraction is larger than 45%; (ii) external and internal stresses are considered to be closely in equilibrium; (iii) the composite strain decreases gradually from the dyke fringes towards its center.

only (Blanchard et al., 1979; Baer, 1995) or a combination between magmatic flow and external pure shear strains with shearing orthogonal to the dyke walls (Smith et al., 1994), a situation not considered here. Asymmetrical fabrics, on the other hand, result mostly from external simple shear strains or a combination between dominant simple and subordinate pure shear strains (Blumenfeld and Bouchez, 1988; Fernandez and Laporte, 1991).

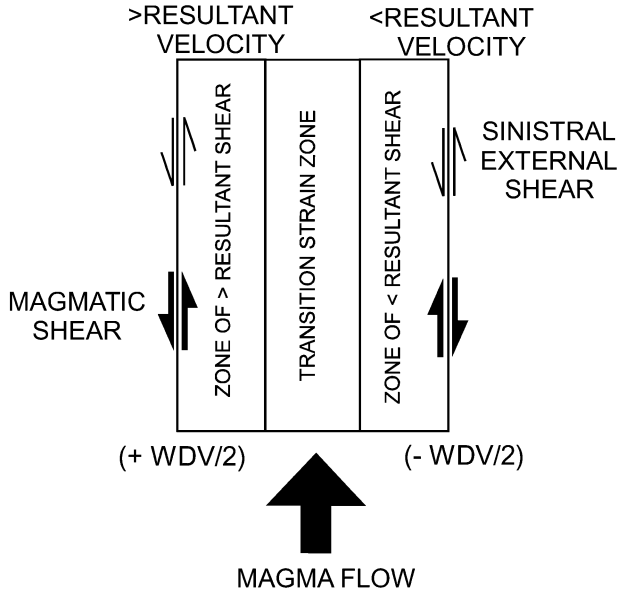

Fig. 6. Schematic three-section division of a hypothetical vertical dyke affected by an external sinistral shear coeval to an internal magmatic shear. Note that one dyke wall moves forwards (with the sense of magma flow) and the other wall moves backwards (counter to the sense of magma flow). Simplifying assumptions imply that the wall displacement velocity (WDV) is divided by two. Positive and negative velocities correspond, respectively, to forward and backward sense of movement with respect to magma flow. The center of the dyke hosts the transition strain zone.

2.2. Idealization of the problem—sufficient conditions

To study the effects and roles of internal and external shear stresses on fabric development in dynamic vertical sheet-like igneous bodies, we shall contemplate the following assumptions (Fig. 5):

(A) *Tectonic setting*: the model comprises any tectonic setting where dykes can be emplaced, irrespective of the bulk kinematic regime in the zone of deformation, the only restriction being that dyke wall displacement vectors must be parallel to magma motion vectors. In order to simplify further field data comparisons, however, the model is focussed on sinistral, pure transcurrent (strike-slip) fault zones.
(B) *Magma and magma flow conditions*: (i) the magma contains a liquid fraction >45% (the 'rigid percolation threshold' (RPT) of Vigneresse et al. (1996)), allowing unhindered displacement and deflection of anisotropic rigid particles within the flow (Blumenfeld and Bouchez, 1988); (ii) for increased concentration of rigid particles, the rotation of individual particles is slowed down or even stopped due to collisions or disturbance of the flow in the matrix caused by neighbours (Blanchard et al., 1979; Ildefonse et al., 1992); (iii) foliations do not rotate past the flow plane, avoiding cyclic evolution of fabrics that are defined by rigid, active markers within a viscous matrix (Fernandez and Laporte, 1991); (iv) the magma flow has a laminar behaviour and moves almost at a constant velocity gradient within the dyke zone 3 (Fig. 2c); and (v) magmatic flow direction is horizontal. The model will also deal with the fact that the flow velocity diminishes from the dyke fringes towards its core (Komar, 1972a,b; Barrière, 1976) (see Fig. 3).
(C) *Stress field*: the internal (magmatic buoyancy-related) and external (tectonic) stress fields are considered to be closely in equilibrium, i.e. the resultant external forces, that we refer to here as principal tectonic stresses, do not exceed the magma pressure within the conduit.
(D) *Strain*: (i) the bulk deformation can be considered in two stages: a pure strain parallel and perpendicular to the dyke walls, followed by a wall-parallel simple shear; (ii) the composite shear strain (magmatic driving shear and simple shear resulting from internal and external forces, respectively) decreases from a maximum at the wall of the dyke to a minimum at the dyke center; (iii) as regards fabrics ellipsoids, the Λ_1 axis is horizontal, the Λ_1–Λ_2 plane is vertical and the fabric ellipses are observed in Λ_1–Λ_3 sections; and (iv) the applied shear strain increases progressively.
(E) *Geometry of the conduit*: the conduit must be vertical and comply with a sheet-like (tabular) geometry. Its walls are taken as regular and smooth, avoiding disturbances in the magma trajectory.

Although this is a large inference, the aim of such

assumptions is to make sure that the effects of the internal (magma) stresses are portrayed mostly by the absolute magma flow velocity (MFV). Likewise, the principal tectonic stress is constrained to control the wall displacement velocity (WDV). Each of the conduit walls will move at the same relative velocity along the same displacement vector but in opposite senses. The absolute WDV will be the sum (in modulus) of the relative velocities of the two sliding walls. Therefore, each wall will move at half of the absolute velocity in relation to the other wall (WDV/2) (Fig. 6).

The concept of dyke walls sliding in opposite senses implies that the wall shifting in the same direction of magma flow will result in less magma-related lateral shear strains at one side of the conduit (e.g. Doblas et al., 1988). Meanwhile, the wall moving in the opposite sense will result in larger lateral shear strains at the other margin. Using this notion and by convention, in relation to the magma flow velocity (MFV; always positive), the side of the conduit wall with forward movement displays a negative velocity divided by two (−WDV), whereas the other shows a positive velocity divided by two (+WDV). Fig. 6 portrays three hypothetical zones of resultant shear within a dyke under coeval internal and external stress.

In order to better illustrate our conceptual model, it is also wise to assume theoretical velocity values for both magma flow and displacement of dyke walls. The magma flow velocity (MFV) will be considered here as 1.0 m/s and constant, on the basis of magma flow rates found in some dyke systems (Delaney, 1987; Pollard, 1987; Turcotte et al., 1987). The relative wall displacement velocity (WDV/2) will be taken as variable and increasing gradually from 0.0 m/s (no displacement) up to 10 m/s (fast displacement), considering intermediate velocities of 0.5, 1.0 and 1.5 m/s.

These conditions are necessary otherwise the problem is much more difficult and not tractable using the methods developed here. While these restrictions put some stringent limits on the practical application of the results, the results obtained provide a substantial amount of insight into the process.

2.3. Predictable model-study cases

Five different cases are predicted in the model (Figs. 7 and 8):

Case 1: MFV $\gg$ WDV/2, where MFV = 1.0 m/s and WDV/2 = 0.0 m/s (Fig. 8a). In this case, the resultant velocities are 1.0 m/s. The fabric ellipses within the conduit are shaped exclusively by the magma flow. The shear strain decreases from the dyke margins to its center, culminating in a symmetric arrangement of fabrics, at the dyke margins, in relation to the dyke symmetry plane (DSP) (Fig. 8a). Therefore, the DSP and the FSP are parallel here, as similarly modelled by Blanchard et al. (1979).

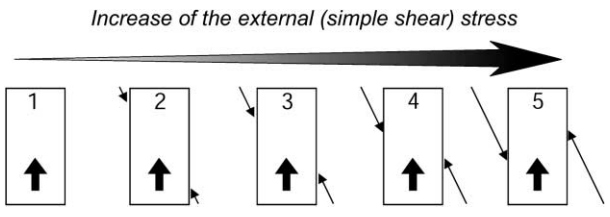

Fig. 7. Possible mechanical variations investigated in this work. From situation 1, only with magmatic flow, to situations 2–5, with progressive increments of external shearing.

Case 2: MFV > WDV, where MFV = 1.0 m/s and WDV/2 = ±0.5 m/s (Fig. 8b). The side of the conduit that slips in the same sense as that of the magma flow displays a resultant velocity of 0.5 m/s. At the other side, where the border slips against the magma flow, the resultant velocity is 1.5 m/s. This perspective yields different fabric ellipses along the dyke. One side of the dyke portrays larger strains than the other. These two different but positive resultant velocities imply that the fabrics will form an acute angle pointing in the same direction as the magma flow (Fig. 8b). The side that hosts larger strains displays fabrics closer to the wall when compared with the side least affected by shearing. The FSP is rotated counter-clockwise in relation to the DSP, that is in the same sense of the strike-slip shearing.

Case 3: MFV = WDV/2 (Fig. 8c). Using these parameters, the resultant velocity is 2.0 m/s. The side of the conduit where the border slips in the opposite sense to that of the magma flow displays a resultant velocity of 0.0 m/s. At the other side, where the border slips along with the magma flow, the resultant velocity is 2.0 m/s. This reasoning implies that one side of the dyke hosts no resultant shear. In this case, the FSP cannot be conceived (Fig. 8c).

Case 4: MFV < WDV/2, where MFV = 1.0 m/s and WDV/2 = ±1.5 m/s (Fig. 8d). The border of the conduit that moves in the same sense as that of the magma flow experiences a resultant velocity of −0.5 m/s—the wall moves faster than the magma. The Λ_1 axis at this side of the dyke composes an obtuse angle with the magma flow plane. The other border moving against the flow shows a resultant velocity of 2.5 m/s. The FSP is rotated clockwise in relation to the DSP, that is, in the opposite sense to the shearing. The angle between the Λ_1 axis and the dyke wall that moves against the flow is smaller in this case than that predicted in Case 2. Fabric orientations, considering those developed on both sides of the dyke, form an acute angle that points against the magma flow (Fig. 8d).

Case 5: MFV $\ll$ WDV/2, where MFV = 1.0 m/s and WDV/2 = ±10.0 m/s (Fig. 8e). In this case, the geometry of the finite fabric ellipses along the conduit is rigorously shaped by external, strike-slip shearing; the influence of the magmatic pressure on the development of kinematic indicators is minimal. The border of the conduit that moves in the same sense of magma flow exhibits a resultant velocity of −9.0 m/s. The other border moving

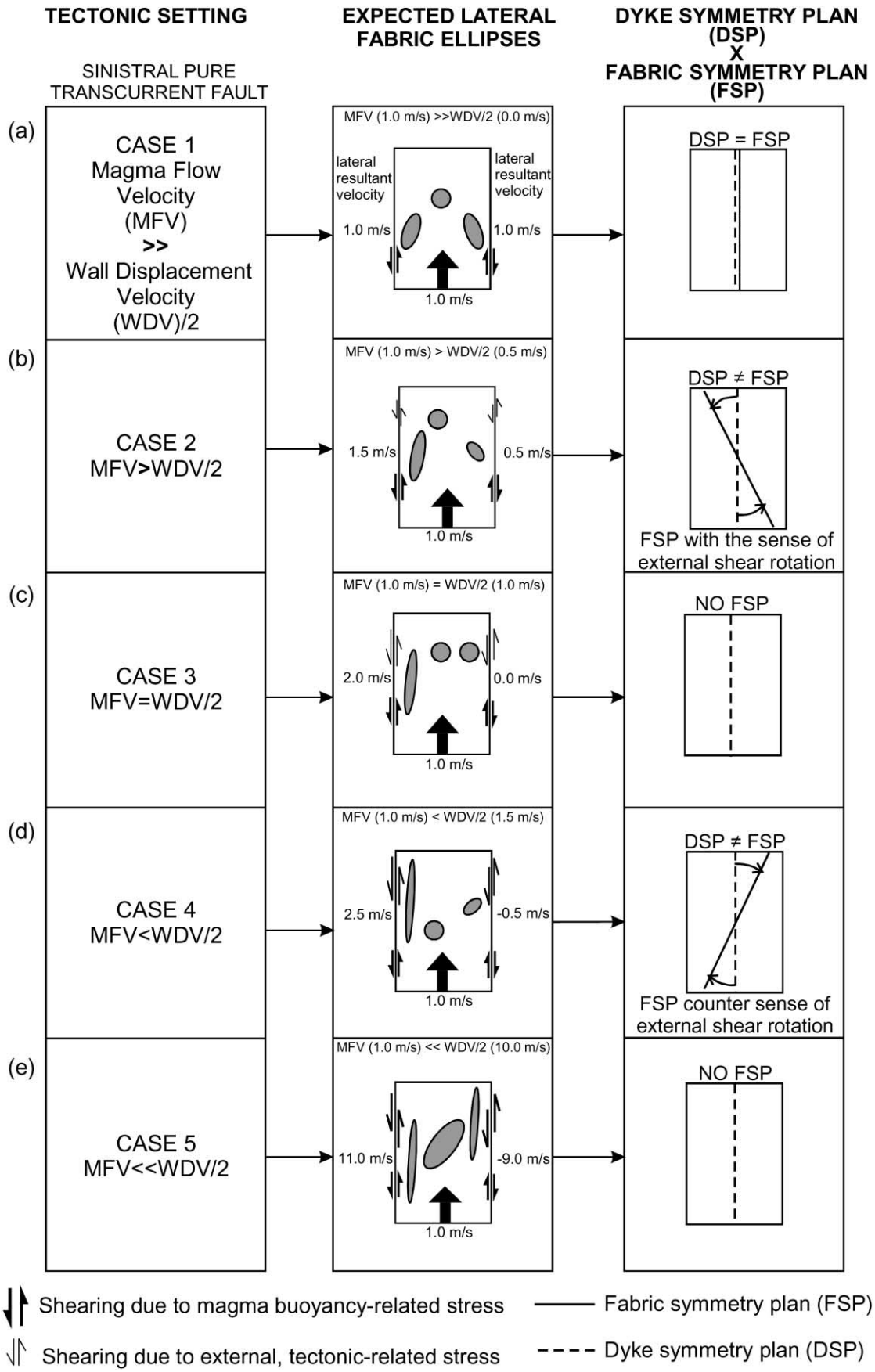
TECTONIC SETTING
EXPECTED LATERAL FABRIC ELLIPSES
DYKE SYMMETRY PLAN (DSP) X FABRIC SYMMETRY PLAN (FSP)
SINISTRAL PURE TRANSCURRENT FAULT
(a)
CASE 1
Magma Flow Velocity (MFV) >> Wall Displacement Velocity (WDV)/2
MFV (1.0 m/s) >>WDV/2 (0.0 m/s)
lateral resultant velocity
lateral resultant velocity
1.0 m/s
1.0 m/s
1.0 m/s
DSP = FSP
(b)
CASE 2
MFV>WDV/2
MFV (1.0 m/s) > WDV/2 (0.5 m/s)
1.5 m/s
0.5 m/s
1.0 m/s
DSP ≠ FSP
FSP with the sense of external shear rotation
(c)
CASE 3
MFV=WDV/2
MFV (1.0 m/s) = WDV/2 (1.0 m/s)
2.0 m/s
0.0 m/s
1.0 m/s
NO FSP
(d)
CASE 4
MFV<WDV/2
MFV (1.0 m/s) < WDV/2 (1.5 m/s)
2.5 m/s
-0.5 m/s
1.0 m/s
DSP ≠ FSP
FSP counter sense of external shear rotation
(e)
CASE 5
MFV<<WDV/2
MFV (1.0 m/s) << WDV/2 (10.0 m/s)
11.0 m/s
-9.0 m/s
1.0 m/s
NO FSP
Shearing due to magma buoyancy-related stress
Shearing due to external, tectonic-related stress
Fabric symmetry plan (FSP)
Dyke symmetry plan (DSP)

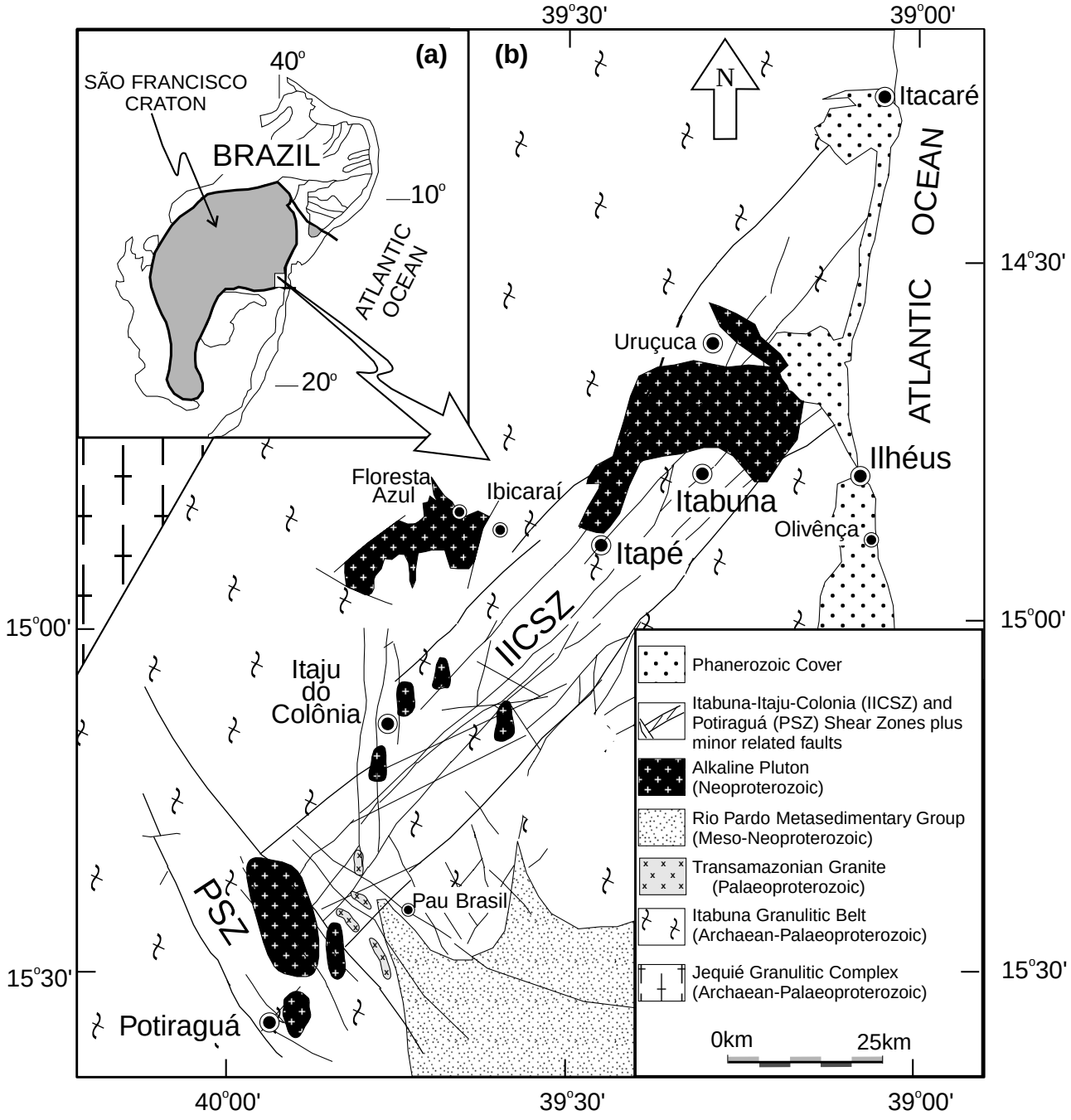

Fig. 9. Locality sketch (a) and geological map (b) of the southeastern terrains of the Bahia State (Barbosa and Dominguez 1996; Correa-Gomes et al., 1998a,b). The Itabuna–Itaju do Colônia Shear Zone (IICSZ) is a major NE–SW structure that crosscuts the Itabuna granulitic belt. PSZ = Potiraguá Shear Zone.

Fig. 8. Idealized cases for coeval performance of shearing induced by external, tectonic-related stress and shearing induced by internal, magma buoyancy-related stress in dykes (left column). The external shear is represented by the wall displacement velocity (in a sinistral pure transcurrent fault zone) and the internal shear by the magma flow velocity. From Case 1 to Case 5, considering a constant magma flow velocity (MFV = 1.0 m/s), half of the wall displacement velocity (WDV/2) increases progressively from 0.0 up to 10.0 m/s. Shapes and positions of fabric ellipses are expected to be unique for each case (central column). The dyke symmetry plan (DSP) and the fabric symmetry plan (FSP) also show different relative positions (right column) for each case, the FSP being absent under some certain conditions (Cases 3 and 5).

against the flow has a resultant velocity of 11.0 m/s. Here, as in Case 3, the FSP cannot be visualized. Contrary to Case 1, where the geometry, displacement and distribution of fabrics is ruled by shearing related to magma flow, in Case 5 we find the other extreme: markers within the conduit are displaced and deflected mostly due to external strike-slip shearing.

In summary, the model implies that under certain circumstances two contrasting kinematics are observed on both dyke borders. On the border moving against the sense of magma flow, obliquities between fabric ellipses and the flow plane are small and decline as fabric ellipses tend to align parallel to the shear plane. On the border moving with the sense magma flow, fabric ellipses form a variable angle with the flow plane. At this side, fabric deformations decrease from Case 1 to Case 3 (where a non-deforming stage is reached), increasing from Case 3 to Case 5, whereas obliquities between fabric ellipses and flow plane increase from Case 1 to Case 2 (acute obliquity) and decrease from Case 4 (obtuse obliquity) to Case 5 (Fig. 8). Therefore, the evolution from Case 2 to Case 3 and Case 4 is crucial to deduce the real magma flow sense in dykes emplaced in active shear fractures.

3. Observational phenomena

Models such as the above provide predictions that can be compared with geological examples, thereby verifying the prediction and, hopefully, simulating new observations of natural phenomena.

3.1. Natural examples: dykes hosted by the Itabuna–Itaju do Colônia Shear Zone, Brazil

We selected a number of dyke segments arranged roughly in parallel patterns that are hosted within a transcurrent, brittle shear zone. This shear zone, named the Itabuna–Itaju do Colônia Shear Zone (IICSZ), is a NE–SW Neoproterozoic structure (150 km by 30 km) that cuts the Archaean–Palaeoproterozoic Itabuna granulitic belt (Barbosa and Dominguez, 1996) at the central-eastern portion of the São Francisco Craton, Bahia State, Brazil (Fig. 9). The IICSZ has a complex tectonic history (Correa-Gomes et al., 1998a) but field evidence shows that all dykes studied in this work were emplaced during sinistral shearing. It is also demonstrable that the source of magma was located to the south in relation to the present position of the studied dykes (Correa-Gomes et al., 1998b) (Fig. 10). Around the city of Itapé (Fig. 9), approximately in the center of the IICSZ, we identified over 300 well-exposed dyke segments, around 1 m thick, usually less than 20 m apart from each other, some of which were considered for this investigation.

Evidences such as the step geometries of dykes, ‘en échelon’ and ‘en relai’ dyke arrangements, displacements

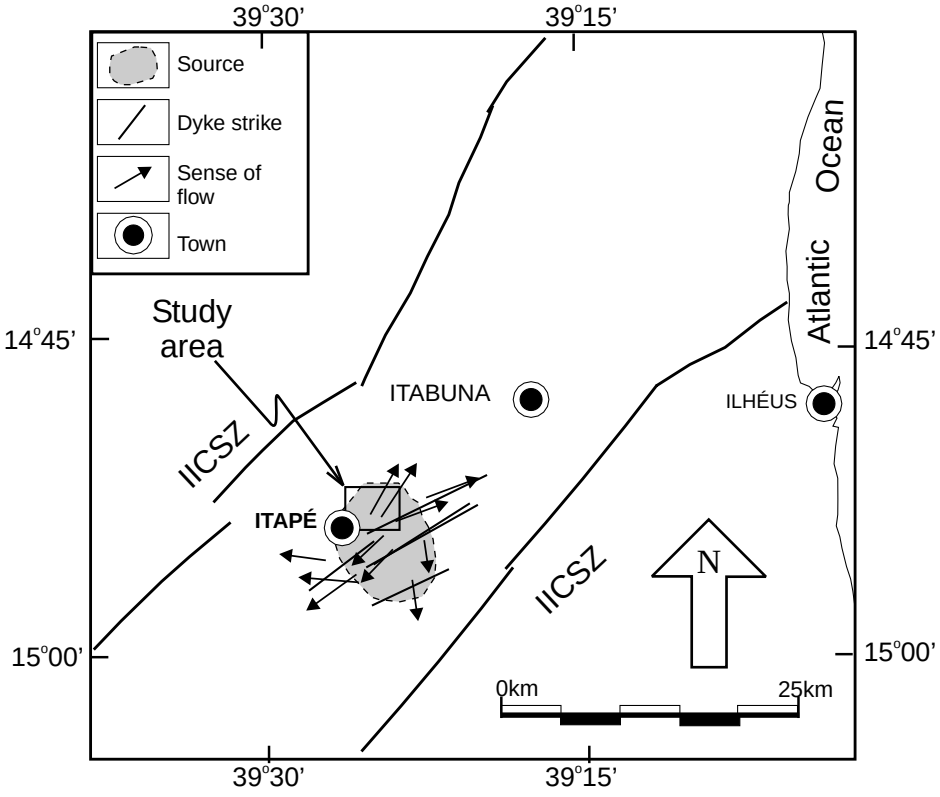

Fig. 10. Sketch map showing the location of the magma source for the studied IICSZ alkaline dykes (modified from Correa-Gomes et al., 1998b).

of external markers (e.g. metamorphic banding) in the dyke walls, similar planar orientation of IICSZ fracture systems and alkaline dyke trends, plus fabrics observed within the dykes, all suggest that the emplacement of these dykes was coeval with the IICSZ tectonic activities (Correa-Gomes et al., 1998a). Some dykes were probably emplaced in several stages, but close in time, during the evolution of the IICSZ.

The dykes show alkaline mafic-to-felsic composition and their ages range from 680 to 550 Ma (de Lima et al., 1981). They are petrogenetic, associated with the Alkaline Suite of Southern Bahia, which comprises silica undersaturated to oversaturated syenitic plutons (Conceição and Otero, 1996). The dykes are composed of phenocrysts of orthoclase and anorthoclase (28–10%), albite and oligoclase (18–2%), hornblende (12–2%), augite (1–0%), magnetite (2–0%) and microlitic groundmass (95–50%). The phenocrysts/matrix proportions correspond, with a good approximation, to the solid/liquid relations suggested in the models.

3.2. Balance between magma buoyancy and tectonic stress fields and magma flow pattern

Field observations indicate that at the time of dyke emplacement, the principal tectonic stresses involved in the IICSZ and the magmatic driving pressure were in equilibrium. Magmatic breccias and shear bands parallel to dyke strikes, usually related to excessive magma pressure, were not observed in the studied dykes, which is consistent with such balance of forces (Pollard 1987; Weinberger et al., 1995).

Although the IICSZ dykes are mostly vertical to subvertical, the studied dykes display plenty of evidence indicating that the flow direction was essentially sub-horizontal and towards the north-northeast. Scour marks, fingers, steps and particle and xenolith arrangements at the edges of the dykes are indicative of horizontal movement of magma within the conduits, features typical of several dyke systems (Rickwood, 1990 and references therein).

3.3. Features used as indicators of magma flow and strike-slip strains

The internal characteristics of a dyke may be of key interest to derive data on magma propagation, flow direction and strain induced by magmatic driving forces. Dykes are noted for the alignment of feldspar phenocrysts and xenoliths, phenomena that have been recognized for many years (Komar 1972a,b; Barrière 1976; Blanchard et al. 1979; Shelley 1985; Smith 1987; Rickwood 1990). The orientation of rigid unequidimensional particles within a magma frozen in after full-crystallization, is thought to be controlled by the laminar flow of the magmatic suspension.

Fig. 11 shows some of the main fabrics related to magmatic flow in sheet-like igneous bodies as described by Smith (1987), Rickwood (1990), Correa-Gomes (1992) and Baer (1995). Though many of these fabrics occur in the study area, the kinematics involved in magma flow were deduced in the IICSZ dykes using mostly the criteria of internal arrangement of xenoliths (mainly those close to wall rocks) and *c*-axes of feldspar phenocrysts, both observed in horizontal planes. Kinematic data collected alongside both dyke walls and at dyke core zones were plotted in 10° intervals in Rose diagrams for structural analysis.

The kinematics and magnitude of external sinistral strike-slip shearing was verified through analysis of the geometry of dyke segments, lateral displacements of local external vertical planar markers (e.g. quartz veins, pegmatites, metamorphic banding), slickensides and steps on the dyke walls (Cadman et al., 1990; Rickwood, 1990; Correa-Gomes, 1992).

3.4. Field analysis

Fig. 12 illustrates five different Neoproterozoic alkaline dykes hosted by the IICSZ that were investigated in the field. Structural features within these dykes provided the following information:

Dyke 1 (Fig. 12a) is a porphyritic mafic dyke segment displaying stepped and bayonet (asymmetric branching) arrangement. Using one dyke branching as a control (see Fig. 12a), we measured 80 *c*-axes of feldspar phenocrysts, which yielded a definite indication of magma flow to the northeast. External markers describe that sinistral strike-slip shearing guided the construction of the conduit. Here, the FSP is rotated counter-clockwise in relation to the DSP, that is in the sense of the external, sinistral strike-slip shearing.

Dyke 2 (Fig. 12b) is a mafic dyke showing stepping features and xenoliths of host rock rotated by the magma flow. The orientations of the long axis of granulite xenoliths indicate that the direction of flow was to the north. Displacement of external markers and thickness variations within the dyke segment (stepping) imply that the dyke was formed along with sinistral strike-slip shearing (e.g. Cadman et al., 1990). As observed in Dyke 1, here the FSP is also rotated counter-clockwise in relation to the DSP, analogous to the sense of the external, sinistral strike-slip shearing.

Dyke 3 (Fig. 12c) includes two parallel mafic dyke segments separated by a bridge of host rock. The geometry of the dyke segments ('en relai' arrangement) and the displacement of external markers define their formation under sinistral strike-slip shearing. These segments also include platy particles of syenitic rock in their interior. We measured 494 xenolith planes and determined that magmatic flow within the dyke was to the northeast. Again, this dyke displays a FSP rotated counter-clockwise in relation to the DSP.

Dyke 4 (Fig. 12d) is a mafic porphyritic dyke segment showing stepping features. These features coupled with

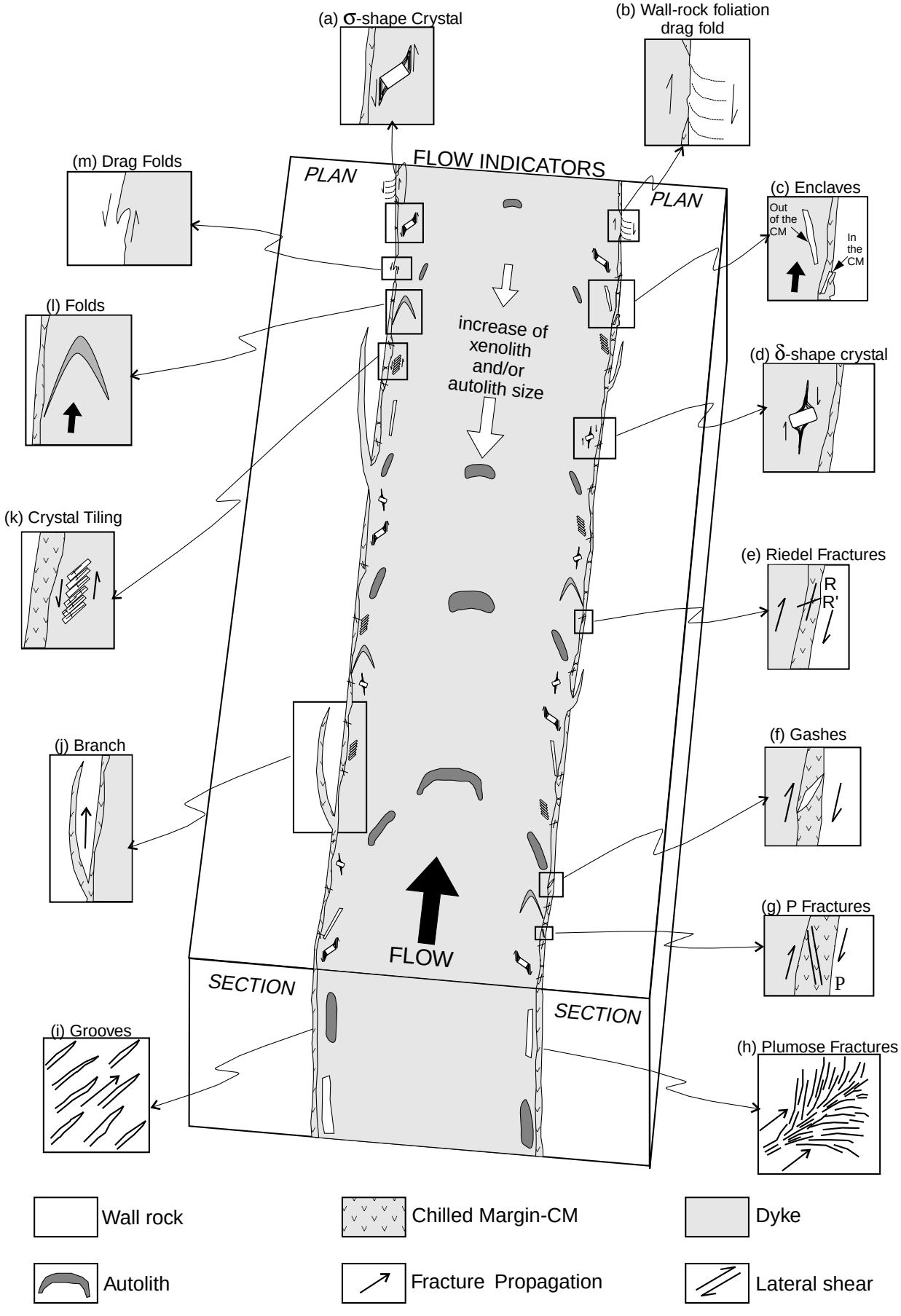
(a) σ-shape Crystal
(b) Wall-rock foliation drag fold
FLOW INDICATORS
PLAN
PLAN
(m) Drag Folds
(c) Enclaves
Out of the CM
In the CM
(l) Folds
increase of xenolith and/or autolith size
(d) δ-shape crystal
(k) Crystal Tiling
(e) Riedel Fractures
R
R'
(j) Branch
(f) Gashes
FLOW
(g) P Fractures
P
SECTION
SECTION
(i) Grooves
(h) Plumose Fractures
Wall rock
Chilled Margin-CM
Dyke
Autolith
Fracture Propagation
Lateral shear

displacement of external planar markers confirm that sinistral strike-slip shearing was coeval with dyke development. We measured 121 *c*-axes of feldspar phenocrysts. Note that from one wall to another, fabrics within the dyke form an acute angle pointing towards the southwest. This indication could be wrongly interpreted as the sense of magma flow, which in fact was toward the north. Such interpretation is based upon three pieces of evidence: (i) the sinistral sense of shear yielded from external markers (i.e. sinistral displacement of quartz veins, pegmatites, metamorphic banding); (ii) the FSP is rotated clockwise in relation to the DSP, which is in contrast with the sense of external shearing; and (iii) the small angles between the Λ_1 axes and the dyke walls (compare the modelled configuration in Case 4 (Fig. 8) with the one approached here (Fig. 12d)).

Dyke 5 (Fig. 12e) is a mafic porphyritic dyke segment. We measured 116 *c*-axes of feldspar phenocrysts, demonstrating that these fabrics are almost parallel to the dyke walls, becoming asymmetric towards the center of the dyke. This suggests that considerable sinistral strike-slip shearing patterned this peculiar arrangement. The FSP is not depicted here.

4. Discussion

The modelling of the geometry and distribution of fabrics within vertical dykes employing concurrent magma buoyancy-related stresses and external, tectonic (strike-slip) stresses proved to be suitable for explaining the kinematics of dykes emplaced within the context of the IICSZ. This work also strongly suggests that the model could be generalized to the understanding of dyke emplacement mechanisms elsewhere, irrespective of the bulk kinematic regime in the zone of deformation.

Our modelled Cases 2 (MFV $>$ WDV/2), 4 (MFV $<$ WDV/2) and 5 (MFV $\ll$ WDV/2) (Fig. 8) were verified in the field, in Dykes 1, 2, 3 (Fig. 12a–c), 4 (Fig. 12d) and 5 (Fig. 12e). Most of the studied dykes fall in Case 2, which is expected in dykes emplaced under external non-coaxial stress fields. Case 1 portrays the 'classic' symmetric distribution of fabrics formed under prominent magma driving pressures. This phenomenon has been widely reported in the literature to occur in dykes typically evolved during insignificant (if any) tectonic shearing parallel to the dyke walls (e.g. volcanic areas and radial dyke systems; Shelley, 1985, 1988; Baer and Reches, 1987; Smith, 1987; Knight and Walker, 1988; Baer 1995). This case was not identified in any of the studied dykes hosted within the transcurrent IICSZ. Case 3, another prediction not yet verified in the field, may prove to be a rare occurrence where the magma flow velocity must match the wall displacement velocity.

5. Implications

This work has a number of important theoretical implications that are supported by our field observations, some of which are addressed below:

- *Palaeostress*: predictions derived from our model imply that kinematic data within dykes, relations between the DSP–FSP and their possible visualization or not in dykes can be used to derive palaeostress data. Statistical analysis of a large number of dykes for their orientations and the tectonically-induced shear senses may provide an indication of local stress fields under which the dykes evolved until their full solidification.
- *Direction of magma flow*: our model demonstrates that angular relations among dyke walls and fabrics and the relations between DSPs and FSPs can be used to determine the direction of magma flow in dykes emplaced within shear fractures. This is an important tool in cases where fabrics may not indicate an unequivocal magma flow direction based on considerations of previous models.

6. Conclusions

Comparisons of what our model predicted with what we observed in the field show a remarkable equivalence and, therefore, we accept that as a reasonable representation of the process. The model sheds light into mechanics of dyke emplacement and evolution not yet fully accessed in previous approaches.

The proposed model and field data indicate that, at least in dykes emplaced in active shear fractures, magma flow direction cannot be unambiguously determined only on the basis of lateral obliquities between flow planes and fabric orientations. This, in fact, requires a combination of fabric obliquities, the mutual geometric relation between DSPs and FSPs and knowledge on the sense of external shearing.

Fig. 11. 3D sketch of some fracture-conduit and macroscopic magma flow fabrics in dykes (adapted from Smith (1987), Rickwood (1990), Correa-Gomes (1992) and Baer (1995)). The dyke is vertical and propagation and flow horizontal. Not all fabrics are necessarily produced concurrently. Some are associated with propagation of a leading fracture system ahead of the dyke and propagation of dyke-tip fluids (e.g. grooves, plumose fractures and some cases of branching), comprising the first and second evolution stages proposed by Baer (1995), though the majority of the fabrics are formed as a function of magma flow within the dyke—that is the third stage (Baer, 1995).

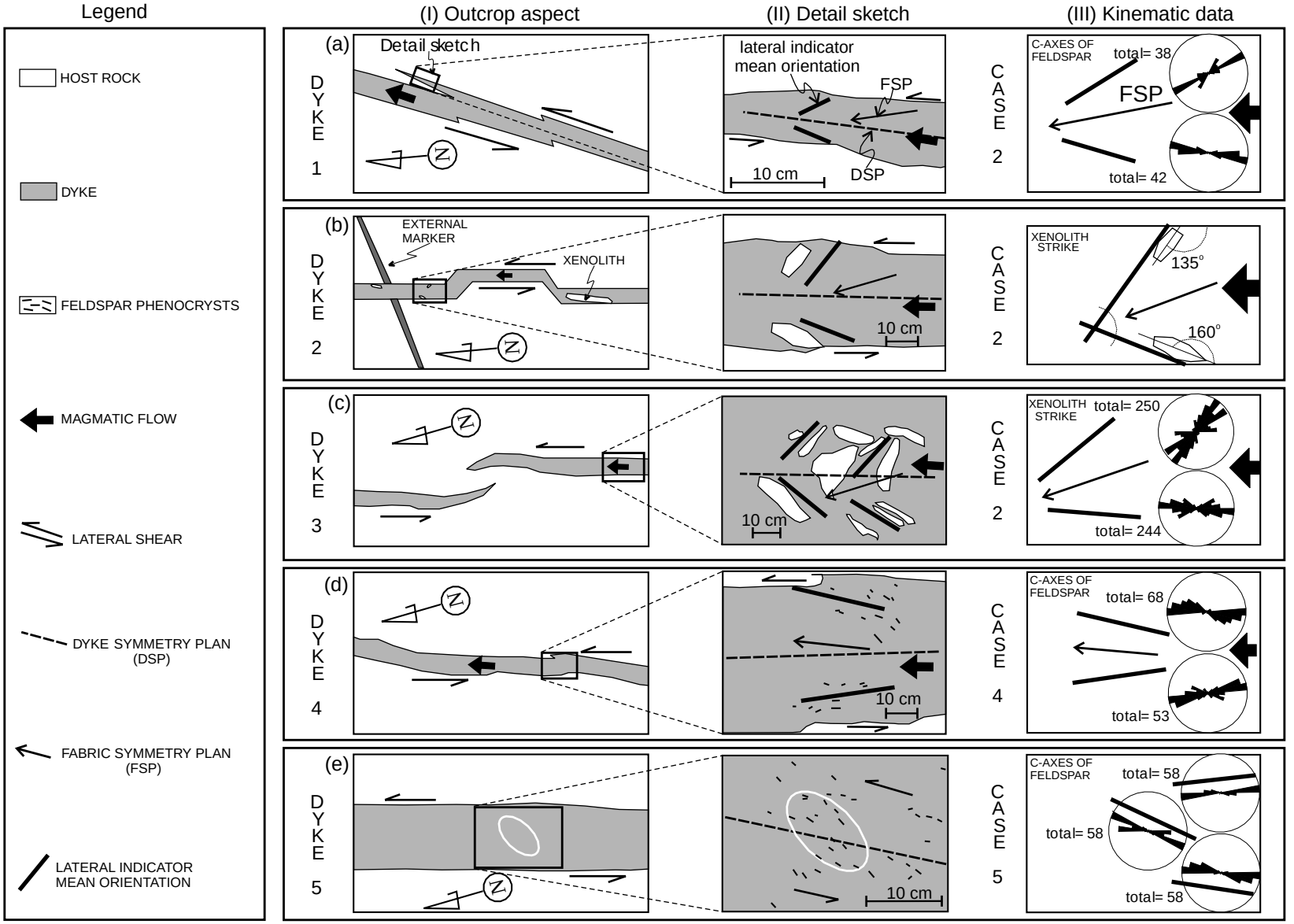

Fig. 12. Five Neoproterozoic alkaline dykes occurring around Itape town that were approached in this study. (a) Outcrop aspect. (b) Inset with detailed sketch of fabric arrangements and orientations, with indication of DSPs and FSPs. (c) Kinematic data: preferred orientation of *c*-axes of feldspars (horizontal projections) and xenoliths (strikes) plotted in Rose diagrams; mean orientation of lateral fabrics and relative position of FSPs.

Acknowledgements

This paper represents our own views on a rapidly expanding body of knowledge about the mechanisms of dyke emplacement. They developed from many discussions, principally with geologists of the University of Campinas (UNICAMP) and Companhia de Pesquisa e Recursos Minerais (CPRM-Bahia State). We thank Professor Brian Windley (Leicester University) for encouraging us to write up this manuscript for publication and Professor Keith Benn (University of Ottawa) for his remarkably helpful review. Fieldwork was supported by FAPESP (Project 96/3582-3). C.R. de Souza Filho and E.P. Oliveira thank CNPq for research grants 301227/94-2 and 300845/91-0, respectively.

References

Arbaret, L., Diot, H., Bouchez, J.-L., 1996. Shape fabrics of particles in low concentration suspensions: 2D analogue experiments and application to tiling in magma. Journal of Structural Geology 18, 941–950.

Baer, G., 1995. Fracture propagation and magma flow in segmented dykes: field evidence and fabric analyses, Maktesh Ramon, Israel. In: Baer, G., Heimann, A.A. (Eds.). Physics and Chemistry of Dykes. Balkema, Rotterdam, pp. 125–140.

Baer, G., Reches, Z., 1987. Flow patterns of magma in dikes, Maktesh Ramon, Israel. Geology 15, 569–572.

Barbosa, J.S.F., Dominguez, J.M.L., 1996. Geologia da Bahia. Texto explicativo para o mapa 1:1,000,000. Salvador, Super. Geol. Recur. Min., SGM, 400p.

Barrière, M., 1976. Flowage differentiation: limitation of the "Bagnold effect" to the narrow intrusions. Contributions to Mineralogy and Petrology 55, 139–145.

Benn, K., Allard, B., 1989. Preferred mineral orientations related to magmatic flow in ophiolite layered gabbros. Journal of Petrology 30, 925–946.

Blanchard, J.P., Boyer, P., Gagny, C., 1979. Un nouveau critère de sens de mise en place dans une caisse filionienne: le "pincement" des minéraux aux éponte. Tectonophysics 53, 1–25.

Blumenfeld, P., Bouchez, J.-L., 1988. Shear criteria in granite and migmatite deformed in the magmatic and solid states. Journal of Structural Geology 10, 361–372.

Cadman, A., Tarney, J., Park, R.G., 1990. Intrusion and crystallization features in proterozoic dyke swarms. In: Parker, A.J., Rickwood, P.C., Tucker, D.H. (Eds.). Mafic Dykes and Emplacement Mechanisms. pp. 13–24.

Conceição, H., Otero, O.M.F., 1996. Magmatismos granítico e alcalino no estado da Bahia: uma epítome do tema. Salvador, Bahia. Super. Geol. Recur. Min., SGM, 133p.

Correa-Gomes, L.C., 1992.Diques máficos: uma reflexão teórica sobre o tema e o seu uso no entendimento prático da geodinâmica fissural. M.Sc. Thesis, Instituto de Geociências, Universidade Federal da Bahia, 196p.

Correa-Gomes, L.C., de Oliveira, E.P., Barbosa, J.S.F., Silva, P.C.F., 1998a. Tectônica associada à colocação de diques alcalinos félsicos e máficos neoproterozóicos na Zona de Cisalhamento de Itabuna–Itaju do Colônia, Bahia, Brasil. Revista Brasileira de Geociências 28, 497–508.

Correa-Gomes, L.C., de Oliveira, E.P., Barbosa, J.S.F., Tanner de Oliveira, M.A.F., 1998b. Circulação magmática em zonas de cisalhamento: os diques alcalinos neoproterozóicos da Zona de Cisalhamento de Itabuna–Itaju do Colônia, SSE do estado da Bahia, Brasil. Revista Brasileira de Geociências 28, 509–518.

Delaney, P.T., 1987. Heat transfer during emplacement and cooling of mafic dykes. In: Halls, H.C., Fahrig, W.H. (Eds.). Mafic Dyke Swarms, pp. 31–46 Geological Association of Canada, Special Paper 34.

Doblas, M., Ubanell, A.G., Villa-Seca, C., 1988. Deformed porphyry dykes in the Spanish Central System. Rendues della Societá Italiana de Mineralógia e Petrológia 43, 517–524.

Elston, W.E., Smith, E.I., 1970. Determination of flow direction of rhyolitic ash-flow tuffs from fluidal textures. Geological Society of America Bulletin 81, 3393–3406.

Fernandez, A., Laporte, D., 1991. Significance of low symmetry fabrics in magmatic rocks. Journal of Structural Geology 13, 337–347.

Gay, N.G., 1968. Pure shear and simple shear deformation of inhomogeneous viscous fluid. I. Theory. Tectonophysics 5, 211–234.

Ghosh, S.K., Ramberg, H., 1976. Reorientation of inclusions by combination of pure and simple shears. Tectonophysics 34, 1–70.

Hanmer, S., Passchier, C.W., 1991. Shear sense indicators: a review. Geological Survey of Canada Papers 90, 1–71.

Hippert, J.F.M., 1993. "V"-pull-apart microstructures: a new shear sense indicator. Journal of Structural Geology 15, 1393–1404.

Hoek, J.D., 1995. Dyke propagation and arrest in Proterozoic tholeiitic dyke swarms, Vestfold Hills, East Antarctica. In: Baer, G., Heimann, A. (Eds.). Physics and Chemistry of Dykes. Balkema, Rotterdam, pp. 79–93.

Ildefonse, B., Launeau, P., Bouchez, J.-L., Fernandez, A., 1992. Effect of mechanical interactions on the development of shape preferred orientations: a two-dimensional experimental approach. Journal of Structural Geology 14, 73–83.

Johnson, A.M., Pollard, D.D., 1973a. Mechanics of growth of some laccolithic intrusions in the Henry Mountains, Utah. I: field observations, Gilbert's Model, physical properties and magma flow. Tectonophysics 18, 261–309.

Johnson, A.M., Pollard, D.D., 1973b. Mechanics of growth of some laccolithic intrusions in the Henry Mountains, Utah. II: bending and failure of overburden layers and sill formation. Tectonophysics 18, 311–354.

Knight, M.D., Walker, G.P.L., 1988. Magma flow directions in dikes of the Koolau Complex, Oahu, determined from magnetic fabric studies. Journal of Geophysical Research 93, 4301–4319.

Komar, P.D., 1972a. Mechanical interactions of phenocrystals and flow differentiation of igneous dikes and sills. Geological Society of America Bulletin 83, 973–988.

Komar, P.D., 1972b. Flow differentiation in igneous dikes and sills: profiles of velocity and phenocrystals concentration. Geological Society of America Bulletin 83, 3443–3448.

de Lima, M.I.C., da Fonseca, E.G., de Oliveira, E.P., Ghignome, J.I., Rocha, R.M., da Carmo, U.F., da Silva, J.M.R., Siga Jr, O., 1981. Folha Salvador (SD.24). Geologia, Texto explicativo 24, 27–192 Levant. Rec. Natur., Projeto Radambrasil, MME, Brasília.

Merle, O., 1998. Internal strain within lava flows from analogue modelling. Journal of Volcanology and Geothermal Research 81, 189–206.

Passchier, C.W., 1994. Mixing in flow perturbations: a model for development of mantled porphyroclasts in mylonites. Journal of Structural Geology 16, 733–736.

Passchier, C.W., Simpson, C., 1986. Porphyroclast system as kinematic indicators. Journal of Structural Geology 8, 831–844.

Philpotts, A.R., Asher, P.M., 1994. Magmatic flow-directions indicators in a giant diabase feeder dike, Connecticut. Geology 22, 363–366.

Pollard, D.D., 1987. Elementary fracture mechanics applied to the structural interpretation of dykes. In: Halls, H.C., Fahig, W.F. (Eds.). Mafic Dyke Swarms. , pp. 5–24 Geological Association of Canada, Special Paper 34.

Ramsay, J.G., 1980. Shear zone geometry: a review. Journal of Structural Geology 2, 83–89.

Rickwood, P.C., 1990. The anatomy of a dyke and the determination of propagation and magma flow. In: Parker, A.J., Rickwood, P.C., Tucker, D.H. (Eds.). Mafic Dykes and Emplacement Mechanisms. , pp. 81–100.

Shaw, H.R., 1969. Rheology of basalt in the melting range. Journal of Petrology 10, 510–535.

Shaw, H.R., Wright, T.Z., Peck, D.L., Okamura, R., 1968. The viscosity of

basaltic magma: an analysis of field measurements in Makuopuni Lava Lake, Hawaii. American Journal of Science 266, 225–264.

Shelley, D., 1985. Determining the paleo-flow directions from groundmass fabric in the Lyttelton radial dykes, New Zealand. Journal of Volcanology and Geothermal Research 25, 69–79.

Shelley, D., 1988. Radial dykes of Lyttelton Volcano—their structure, form and petrography, New Zealand. Journal of Geology and Geophysics 31, 65–75.

Simpson, C., Schmid, S.M., 1983. An evaluation of criteria to determine the sense of movement in sheared rocks. Bulletin of the Geological Society of America 94, 1281–1288.

Smith, R.P., 1987. Dyke emplacement at the Spanish Peaks, Colorado. In: Halls, H.C., Fahrig, W.H. (Eds.). Mafic Dyke Swarms. , pp. 47–54 Geological Association of Canada, Special Paper 34.

Smith, J.V., Yamauchi, S., Miyake, Y., 1994. Coaxial progressive deformation textures in extrusive and shallow intrusive rocks, Southwest Japan. Journal of Structural Geology 16, 315–322.

Turcotte, D.L., Emerman, S.H., Spence, D.A., 1987. Mechanics of dyke injection. In: Halls, H.C., Fahrig, W.H. (Eds.). Mafic Dyke Swarms, pp. 20–25 Geological Society of Canada, Special Paper 34.

Weinberger, R., Baer, B., Shamir, G., Agnon, A., 1995. Deformation bands associated with dyke propagation in porous sandstone, Maktesh Ramon, Israel. In: Baer, G., Heimann, A. (Eds.). Physics and Chemistry of Dykes. Balkema, Rotterdam, pp. 95–112.